Russian Academy of Sciences
Joint Institute for High Temperatures RAS
Institute of Problems of Chemical Physics RAS
Kabardino-Balkarian State University

# Physics of Extreme States of Matter — 2013

Moscow, 2013

# Physics of Extreme States of Matter — 2013

Edited by academician Fortov V. E., Karamurzov B. S., Efremov V. P., Khishchenko K. V., Sultanov V. G., Levashov P. R., Andreev N. E., Kanel G. I., Iosilevskiy I. L., Milyavskiy V. V., Mintsev V. B., Petrov O. F., Savintsev A. P., Shpatakovskaya G. V.

This compendium is devoted to investigations in the fields of physics of high energy densities and thermal physics of extreme states of matter. Interaction of intense laser, x-ray and microwave radiation, powerful particle beams with matter, techniques of intense energy fluxes generation, experimental methods of diagnostics of ultra-fast processes, physics of shock and detonation waves, different models and results of theoretical calculations of equations of state for materials at high pressures and temperatures, low-temperature plasma physics, issues of physics and power engineering, as well as technology projects are considered. The majority of the works has been presented at the XXVIII International Conference on Interaction of Intense Energy Fluxes with Matter (March 1–6, 2013, Elbrus, Kabardino-Balkaria, Russia). The edition is intended for specialists in physical and technical problems of power engineering.

ISBN 978-5-94691-533-5

# CONTENTS

## *CHAPTER 1. POWER INTERACTION WITH MATTER*



## *CHAPTER 2. SHOCK WAVES. DETONATION. COMBUSTION*

## *CHAPTER 3. EQUATIONS OF STATE FOR MATTER*



## *CHAPTER 4. PHYSICS OF LOW TEMPERATURE PLASMA*

**Conclusion.** In connection with the problem of laser simulation of impact processes, we note that in our case, ablation pressure on the andesite target was $\sim 4{\cdot}10^6$ atm at I$\sim 10^{13}$ W/cm$^2$. A typical resulting pressure in case of micrometeorite impact (mass $10^{-13}$ g) is of the order of $E/[(4/3)\pi d_m^2] \sim \rho_m V^2$ [6]. It follows that these experiments could simulate a collision with velocities around 13 km/s.


1. Guskov S. Y., Borodzyuk S. *et al.* // Quantum Electronics. 2004. V. 34. No. 11. P. 989.
2. Kozlowski E. A. Mountain Encyclopedia M.: Soviet Encyclopedia, 1991 [in Russian].
3. Burdonsky I. N.,Leonov A. G., Timofeev I. S. *et al.*// Investigated in Russia. 2012. V. 42. P. 574.
4. Mora P.// Phys. Fluids. 1982. V. 25. P. 1051.
5. Zel'dovich B., Raiser Y. P. // Physics of shock waves and high-temperature hydrodynamic phenomena. M.:Science, 1968 [in Russian].
6. Stanyukovich K. P. //Unsteady motion of a continuous medium. M.:Science, 1971 [in Russian].


## KINETIC COEFFICIENTS OF METALS ABLATED UNDER THE ACTION OF FEMTOSECOND LASER PULSES


***Petrov Y. V.,*[1] *Inogamov N. A.,*[1] *Migdal K. P.*[2]**

[1]*ITP RAS, Chernogolovka,* [2]*VNIIA, Moscow, Russia*

**uvp49@mail.ru*



Kinetic coefficients of metals in two-temperature state arising under the action of femtosecond laser pulses are calculated in dependence on electron temperature. Among metals, used as targets for the investigation of their ablation under the action of laser irradiation, simple, with s- and p-electrons, as well as noble and transition metals with laser-excited d-electrons are considered.



*Keywords:* femtosecond laser ablation, kinetic coefficients


**Introduction.** Dynamics of ablation of metals under the action of ultrashort laser pulses essentially depends upon their transport properties such as electron thermal conductivity and energy exchange between electrons and ions. At the early stage of laser pulse-metal target interaction the metal state can be characterized by electron and ion temperatures, which differ to a great extent from one another, and by the minor change of a target volume. Electron kinetic characteristics of a metal define the depth of the surface layer of a metal target heated by the laser pulse. This heated layer is produced by the electron heat propagation and heat trans mission from electrons to ions resulting in the equalization of electron and ion temperatures. Because of its high temperature, target surface layer has a high pressure giving rise to the onset of ablation. We have calculated electron heat conductivity coefficient and electron-phonon coupling factor, governing the electron-ion energy relaxation. Among metals used as the targets, when laser ablation is investigated, we consider metals with dif- ferent electron energy bands: simple metals with only s- and p- electrons excited under the action of laser irradiation and also rare and transition metals with laser-excited d-electrons.

**Electron-ion scattering frequencies.** According to the two-temperature approach, we suggest that phonons (in the Debye approximation) are described by their partition function in dependence of their momentum $\mathbf{q}$ as $N(q) = [e^{\hbar\omega_\mathbf{q}/k_B T_i} - 1]^{-1}$ with the ion temperature $T_i$ different from the electron temperature $T_e$. Electron temperature $T_e$ define Fermi partition function of s-, p- electrons (commonly called by s-electrons) and d-electrons with the dispersion laws

$$\varepsilon(\mathbf{p}) = \varepsilon_s + p^2/2m_s, \quad \varepsilon(\mathbf{p}') = \varepsilon_1 + p'^2/2m_d. \qquad (1)$$

and effective masses $m_s$ and $m_d$. d-electron energy lies within the d-band width $\varepsilon_1 \le \varepsilon(\mathbf{p}') \le \varepsilon_2$. Parabolic dispersion law for s- and d-electrons approximates

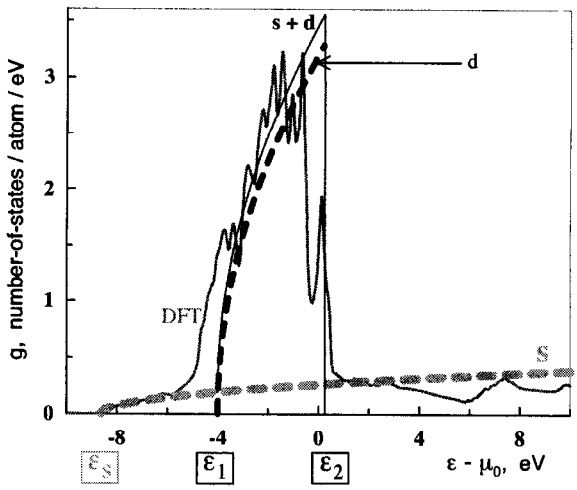


**Figure 1.** Ni density of state, obtained by the density functional method and parabolic approximation of the density of state of s- and d-electrons.

more real energy spectra and electron density of state which we obtained for metals under consideration by the density functional method [1]. Results of density functional theory application and parabolic approach for the density of state of Ni are presented in Fig.1.

Ion temperature $T_i$ in our calculation lies within the interval from the Debye temperature $\theta$ to the temperature value $T_\star$ of the order of several melting temperature $T_m$. In single temperature (1T) case ($T_e = T_i = T$), when $\theta < T < T_\star$, electron heat conductivity coefficient $\kappa_{1T} = \kappa(T)$ is defined by the electron-ion scattering (e-e collisions give negligible contribution under these conditions).

In Fig. 2 experimental data on dependence of the resistivity of some noble and transition metals on the temperature in single temperature case is shown. These experimental data are obtained in modern mea-

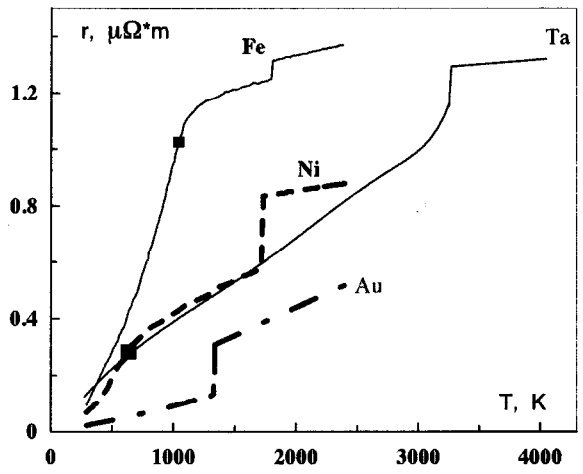


**Figure 2.** Dependence $r(T)$ of the resistivity of some noble and transition metals on the temperature in the single temperature case.

surements of resistivity of thin wires, heated by the electric current pulse [2]. Experiments of this kind allows to reach the temperature values much more than the melting temperature. In solid state of pure metals above the Debye temperature resistivity $r$ increases proportionally to $T$ increase because of the phonon number growth. In magnetic metals (Ni, Fe in Fig. 2) linear rise of resistivity lasts up to Curie temperature (squares in Fig.2). For the iron this linear on $T$ dependence takes place at large resistivity values, comparable with the limit metallic resistivity $r_{m,m} \sim m_e v_F/n_s e^2 a \sim \hbar a/e^2 \sim 1$ $\mu\Omega$·m; here the collision frequency $\nu$ has its maximum value of the order of $v_F/a$, where $v_F$ is the Fermi velocity, $a$ is the lattice constant.

We take into account the change of the slope of $r(T)$ curves after the melting and their approach the maximum metallic values by writing the resistivity via its linear approximation $r_s = a + bT$ before melting and this limit metallic resistivity $r_{m,m}$ as the interpolation expression $r(T_i) = (r_s^{-2} + r_{m,m}^{-2})^{-1/2}$. The resistivity obtained by this means define the effective electron-ion collision frequency as a function of the ion temperature from the Drude relation:

$$\nu_{si} = \frac{n_s(T_e)\, e^2 r(T_i)}{m_s}. \qquad (2)$$

Here $n_s(T_e)$ is the concentration of s-electrons, depending upon the electron temperature because of the excitation of d-electrons into the s-band.

**s-s and s-d electron-electron scattering.** Effective frequency of s-electron collisions with other electrons $\nu_{se}$ in metals with d-electrons can be written as $\nu_{se} = \nu_{ss} + \nu_{sd}$, with consequently s-s collision frequency $\nu_{ss}$ and s-d collision frequency $\nu_{sd}$. Influence of s-s electron scattering onto the electron heat conductivity of simple metals was considered in [3]. Additional effective frequency of scattering of s-electrons on d-electrons is now calculated by the following manner. First we calculate the depending upon the s-electron momentum $\mathbf{p}$ its collision frequency $\nu_{sd}(\mathbf{p})$. It can be written as

$$\nu_{sd}(\mathbf{p}) = \frac{2\pi}{\hbar} \int \frac{u^2(q)\, d^3q}{(2\pi\hbar)^3} \int \frac{2d^3p\prime}{(2\pi\hbar)^3} S\, \delta. \qquad (3)$$

Here s-electron having the momentum $\mathbf{p}$ interacts with d-electron having the momentum $\mathbf{p}\prime$. $\mathbf{q}$ is a transferred momentum. Function

$$\delta = \delta[\varepsilon(\mathbf{p}) + \varepsilon\prime(\mathbf{p}\prime) - \varepsilon(\mathbf{p}+\mathbf{q}) - \varepsilon\prime(\mathbf{p}\prime - \mathbf{q})].$$

stands for the energy conservation. Statistical factor $S$ in (3) has the form

$$S(\mathbf{p}, \mathbf{p}\prime, \mathbf{q}) = f_d(\mathbf{p}\prime)[1 - f_s(\mathbf{p}+\mathbf{q})][1 - f_d(\mathbf{p}\prime - \mathbf{q})] +$$

$$+ f_s(\mathbf{p}+\mathbf{q}) f_d(\mathbf{p}\prime - \mathbf{q})[1 - f_d(\mathbf{p}\prime)],$$

where $f_s$ and $f_d$ are Fermi distribution functions of s- and d-electrons with the chemical potential $\mu$. Equation (3) includes a Fourier transform $u(q)$ of electron-electron screened Coulomb interaction $u(r) = e^2 \exp(-r/\lambda)/r$, where $\lambda(T_e)$ is the screening length in Thomas-Fermi approximation [4, 5]. Frequency $\nu_{sd}(\mathbf{p})$ obtained from (3) is then used to calculate the heat conduction coefficient $\kappa_{sd}(T_e)$, due to the s-d scattering. Within the $\tau$- approach

$$\kappa_{sd} = \int (\varepsilon - \mu)(-f_s') \left(\mu' + \frac{\varepsilon - \mu}{T_e}\right) \frac{v_s^2(p)}{\nu_{sd}(p)} \frac{p^2 dp}{3\pi^2\hbar^3}, \qquad (4)$$

where $f_s' = \partial f_s(\varepsilon)/\partial\varepsilon$, $\mu' = \partial\mu/\partial T_e$, $v_s(p)$ is the velocity of s-electron. Sixfold integration in (3) is reduced to double integration in $q = |\mathbf{q}|, p' = |\mathbf{p}'|$ - plane. Taking it into account, expression (4) can be written as a threefold integral over $p', q$ and $p$. Effective frequencies $\nu_{sd}(T_e)$ then can be defined as those to give the same value of the heat conductivity coefficient $\kappa_{sd}$ from the Drude formula: $\nu_{sd} = C_s \bar{v}_s^2/3\kappa_{sd}$. Analogously effective s-s collision frequency $\nu_{ss} = C_s \bar{v}_s^2/3\kappa_{ss}$.

Effective s-electron collision frequencies $\nu_{se}(T_e) = \nu_{ss} + \nu_{sd}$ for some simple, noble and transition metals are presented in Fig. 3. As it can be seen, at electron temperatures $T_e$ under consideration s-e contribution exceeds that one from s-i scattering only at ion temperatures $T_i$ less than $\sim$ 1 kK. Depending upon electron and ion temperatures electron heat conductivity coefficient $\kappa(T_e, T_i)$, taking into account s-i , s-s and s-d scattering, is shown in Fig. 4 for $T_i$ to be a room temperature. Fig. 5 illustarates dependence on the electron temperature of the heat conductivity coefficient of nickel at different values of ion temperature $T_i$.

**The rate of electron-ion heat transfer.** The energy transferred from electrons to ions in the unit volume in the unit time can be written as [6]

$$\dot{E} = \int \hbar\omega_{\mathbf{q}} \dot{N}_{\mathbf{q}} V\, d\mathbf{q}/(2\pi\hbar)^3 = \alpha(T_e)\,(T_e - T_i). \qquad (5)$$

Expression (5) defines the electron-phonon coupling factor $\alpha$. The quantity

$$\dot{N}_{\mathbf{q}} = 2 \int \Phi\, W_{\mathbf{q}}\, \delta(\varepsilon_{\mathbf{p}-\mathbf{q}} + \hbar\omega_{\mathbf{q}} - \varepsilon_{\mathbf{p}})\, d\mathbf{p}/(2\pi\hbar)^3$$

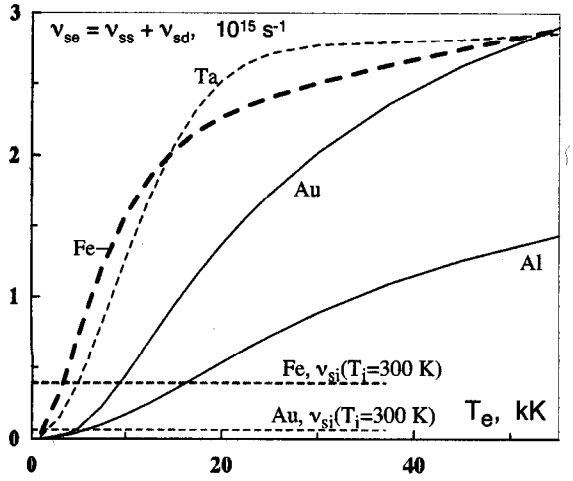


**Figure 3.** Effective collision frequency of s-electrons with other electrons in some simple, noble and transition metals. Horizontal lines stand for the electron-ion collision frequencies of Au and Fe at the ion temperature $T_i = 300$ K.

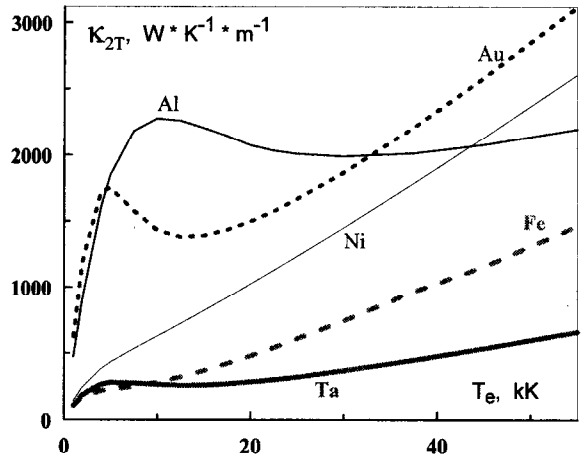


**Figure 4.** s-electron heat conductivity coefficient $\kappa(T_e, T_i)$ for simple (Al), noble(Au) and transition (Ni, Fe, Ta) metals. Ion temperature $T_i = 300$ K.

in equation (5) is a rate of change of longitudinal phonons with momentum $\mathbf{q}$ and energy $\hbar\omega_{\mathbf{q}}$ concentration $N_{\mathbf{q}}(t)$.

$$\Phi = (1 - f_{\mathbf{p}-\mathbf{q}}) f_{\mathbf{p}} + N(\mathbf{q})[(1 - f_{\mathbf{p}-\mathbf{q}}) f_{\mathbf{p}} - (1 - f_{\mathbf{p}})\, f_{\mathbf{p}-\mathbf{q}}]$$

is the statistical factor with Fermi $f_{\mathbf{p}}$ and Bose $N(\mathbf{q})$ distribution functions. Phonon frequencies are taken in the Debye approach: $\omega_{\mathbf{q}} = c_s\,|\mathbf{q}|/\hbar$. Probability for the electron in the metal to change the momentum from $\mathbf{p}$ to $\mathbf{p} - \mathbf{q}$ in a unit time under the interaction with longitudinal phonons is

$$W_{\mathbf{q}}\, \delta(\varepsilon_{\mathbf{p}-\mathbf{q}} + \hbar\omega_{\mathbf{q}} - \varepsilon_{\mathbf{p}})$$

with

$$W_{\mathbf{q}} = \pi\omega_{\mathbf{q}}/(\rho V c_s^2) \cdot n_{at}^2 U^2(\mathbf{q})$$

Here $U(\mathbf{q}) = 4\pi e^2\hbar^2 Z_i/(q^2\epsilon(\mathbf{q}))$, and $\epsilon(\mathbf{q})$ is the dielectric permeability in the Lindhard approach [4, 5],

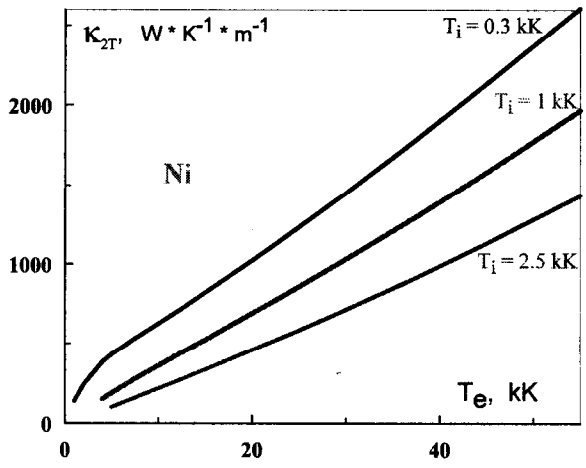


**Figure 5.** s-electron heat conductivity coefficient $\kappa(T_e, T_i)$ of nickel. Ion temperatures in kK above the curves correspond both to solid and liquid states.

$Z_i$ is the effective charge of ion, $n_{at}$ - concentration of atoms, $\rho$ - mass density. Total electron-phonon coupling factor in (5) is a sum of separate s- and d-electron factors $\alpha_s$ and $\alpha_d$ : $\alpha = \alpha_s + \alpha_d$. For the case of $\alpha_s$ the effective ion charge $Z_i = n_s(T_e)/n_{at}$, and in $\alpha_d$ case $Z_i = Z_s(T_e) + Z_d(T_e)$ =const. Electron-phonon coupling factor $\alpha_d$ can be written as

$$\alpha_d = \frac{m_d^2}{4\pi^3\hbar^7}\,\frac{k_B^2 T_e}{\rho\, c_s} \times \int_0^{q_D} dq \cdot q^2\, U^2(\mathbf{q}) \ln\frac{e_1 + e_2}{e_1 + 1}\Big|_{\varepsilon=a}^{\varepsilon=b}, \quad (6)$$

with

$$e_1 = \exp\frac{\varepsilon - \mu - \hbar\omega_q}{k_B T_e}, \quad e_2 = \exp\left(-\frac{\hbar\omega_q}{k_B T_e}\right),$$

$$a = \varepsilon_1 + \frac{1}{2m_d}\left(\frac{q}{2} + m_d c_s\right)^2, \quad b = \varepsilon_1 + \frac{p_d^2}{2m_d},$$

$q_D$ is the Debye momentum. Electron-phonon coupling factor $\alpha_s$ is expresed by the formula, similar to (6). At temperatures exceeding the Debye temperature $\alpha$ depends only on the electron temperature but not the ion temperature. As a function of electron temperature it is shown in Fig. 6 for aluminum (simple metal) and gold (noble metal). Curves $Au_1$ and $Au_{0.6}$ differ by the value of the effective mass of s-electrons (1 and 0.6 a.u. correspondently). Curve $Au_{corr}$ is obtained by the multiplying $Au_{0.6}$ by the factor reducing $\alpha$ to the experimental value [7–9] at the room temperature.

Analogously electron-phonon coupling factor for transition metals (nickel, iron and tantalum) as a function of electron temperature is presented in Fig.7.

Fig. 6 demonstrates the significant increase of electron-phonon coupling factor with electron temperature growth in gold, similar to the results of the works [10, 11]. Of partial electron-phonon coupling factors $\alpha_s$ and $\alpha_d$ in this noble metal $\alpha_d$ dominantly contributes to the total $\alpha$ at electron temperatures greater than 5 kK.

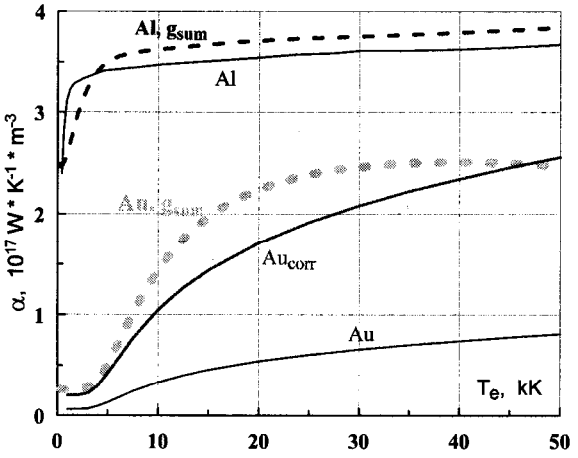


**Figure 6.** Electron-phonon coupling factor $\alpha(T_e)$ of Al and Au in dependence on the electron temperature. Comparison is made with the work [11] data (marked by $g_{sum}$).

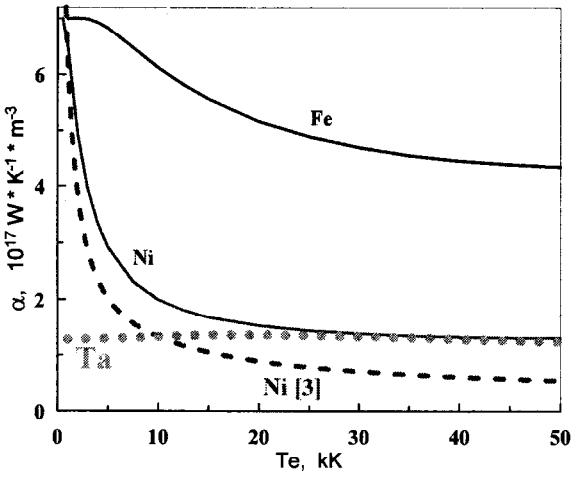


**Figure 7.** Electron-phonon coupling factor of transition metals (Ni, Fe and Ta ) in dependence on the electron temperature. The curve Ni[3] is taken from the work[11].

In the case of transition metals $\alpha_d$ gives the main contribution into the full electron-phonon coupling factor at all electron temperatures $T_e$. Different transition metals differ with respect to the position of Fermi level within the d-band. Three typical cases can be observed: a) Fermi level is slightly (several percents of d-band width) lower than the upper edge of d-band; b) difference between Fermi level and the upper edge of d-band has the moderate value of the order of ten percents of d-band width; c) Fermi level is essentially lies within the d-band. Band structure of Ni belongs to the case a). Here we can see a drastic decrease of $\alpha(T_e)$ coefficient at $k_B T_e > \varepsilon_2$. In the case b) (it is presented by Fe) the $\alpha(T_e)$ decrease with electron temperature increase has a smooth fall character. And in the last case, when the Fermi level lies within the d-band (Ta), $\alpha(T_e)$ function is approximately constant.

**Acknowledgments.** The authors are grateful to RFBR grant 11–08–01116–a and RAS Presidium Program "Matter at high energy density" for the financial support.

1. Yu.V. Petrov, N.A. Inogamov, K.P. Migdal, Pis'ma v ZhETF **97**(1), 24 (2013).
2. G. Pottlacher, *High Temperature Thermophysical Properties of 22 Pure Metals,* Keiper (2010).
3. N.A. Inogamov, Yu.V. Petrov, JETP, 110(3), 446–468 (2010).
4. J.M. Ziman, *Principles of the Theory of Solids,* Cambridge, The University Press (1972).
5. W.A. Harrison, *Solid State Theory,* McGraw-Hill, New York, London, Toronto (1970).
6. M.I. Kaganov, I.M. Lifshitz, L.V. Tanatarov, ZhETF **31**, 232 (1956).
7. Weigang Ma, Haidong Wang, Xing Zhang, Wei Wang, Int. J. Thermophys. DOI 10.1007/s10765–011–1063–2
8. P.M. Norris, J.L. Hostetler, A.N. Smith, D.M. Czajkowsky, P.M. Norris, Appl. Opt. **38,** 3614 (1999).
9. W.G. Ma, H.D. Wang, X. Zhang, W. Wang, J. Appl. Phys. **108,** 064308 (2010).
10. X.Y. Wang, D.M. Riffe, Y.-S. Lee, M.C. Downer, Phys. Rev. B **50**(11), 8016 (1994).
11. Zh. Lin, L.V. Zhigilei, V. Celli, Phys. Rev. B **77**, 075133 (2008).

## RADIATION RESISTANCE OF SODIUM CHLORIDE FOR SHORT LASER PULSES

***Savintsev A.P.,* Gavasheli Yu.O.***
*KBSU, Nalchik, Russia*
**pnr@kbsu.ru*

In this paper, drawing on the data calculated the radiation resistance of sodium chloride in the range of the laser pulse duration of 1 ps–50 fs. It was found that for $\tau = 200$ fs critical field strength in sodium chloride and other inorganic optically transparent material is practically the same.

*Keywords:* Radiation resistance, sodium chloride, laser pulse duration.

Radiation resistance of optically transparent solids numerically characterized radiation damage threshold (voltage breakdown): critical flux density of optical radiation, from which the volume or on the surface of irreversible changes occur as a result of anomalous absorption of the light flux.

For transparent solids is a certain dependence of the breakdown threshold and, consequently, the radiation resistance of the duration of short laser pulses. The experiments showed that, as a rule, with decreasing pulse radiation resistance increases. Study of the nature of this dependence helps to understand the mechanisms and patterns of breakdown.

This paper was given the task to calculate the values of radiation resistance of sodium chloride in the femtosecond laser pulse duration range.